The Evolving Scholar Vol. 3, 2023 https://dx.doi.org/10.59490/6512dbe88ec0d252c9084caa

Bicycle and Motorcycle Dynamics 2023
Symposium on the Dynamics and Control of Single Track Vehicles
18 – 20 October 2023, Delft University of Technology, The Netherlands

Type of the Paper: Conference Paper

Investigation of the Applicability of a Motorcyclist Model for Trajectory Prediction in Real Traffic

Scherer, F.[1]* and Eschinger, M.[2]

[1]Technical University Darmstadt; florian.scherer@tu-darmstadt.de, https://orcid.org/0009-0007-8234-3347
[2]Technical University Darmstadt, maximilian.eschinger@web.de
*corresponding author.

Name of Editor: Jason Moore
Submitted: 26/09/2023
Accepted: 02/10/2023
Published: 03/10/2023
Citation: Scherer, F. & Eschinger, M. (2023). Investigation of the Applicability of a Motorcyclist Model for Trajectory Prediction in Real Traffic. The Evolving Scholar - BMD 2023, 5th Edition.

Abstract:
To develop advanced motorcycle assistance systems, the focus is shifting towards the rider's abilities. A model in (Scherer et al. 2022) predicts motorcycle dynamics influenced by riders without specific rider or vehicle parameters. It employs mathematical functions to describe speed and roll angle changes, revealing differences among riders. Unlike previous stochastic approaches, this model allows clear interpretation of measurement data with rider-specific parameters like correction amplitudes and trends, aiding critical maneuver identification.

The paper investigates applying this rider model to real traffic data. For this purpose, three riders (two experienced frequent riders and one inexperienced infrequent rider) on two different vehicles (Honda CBF 1000 and BMW K1200R Sport) were recorded and examined on a sample basis using a validated low-cost measurement technique with a total amount of n = 40 measurements. Taking into account evaluation curves suitable for proving the methodology, two consecutive country road curves were selected with a respective change in direction (equivalent to a yaw angle change of the vehicle between entering and exiting the curve) of approx. 180°. These were each driven through 5 times by all three riders under constant conditions in good, summer weather and road conditions. In addition, one of the riders drove through them in wintry and less than optimal road conditions at the beginning of the season.

Initial findings assess the model's transferability to real traffic. The investigation results show its applicability, with rider-specific riding styles and parameterization functions, as well as the need to repeat the study with a large number of samples.

The model accurately predicts future positions, with over 85% of maneuvers having less than a 2% lateral deviation. This demonstrates applicability under real conditions, confirming its efficacy beyond the closed terrain test in (Scherer et. al., 2022).

In the future, this model will enable rider-dependent trajectory predictions with uncertainty intervals in real traffic situations.

Keywords: Trajectory, Motorcycle, Modeling, Study, Real Traffic, Simulation, Dynamics, Riding Ability, Parameterisation

ISSN: 2667-2812

 http://dx.doi.org/10.59490/6512dbe88ec0d252c9084caa

Introduction

The accident statistics show that 33.7 % of all motorcycle accidents in 2020 can be classified as single-vehicle accidents. Motorcyclists between the ages of 15 and 24 are the most affected age group, accounting for more than one third of all riders involved in accidents. The most frequent cause of accidents involving motorbikes with registration plates was found to be "inappropriate speed" in 22.4 % of cases (Destatis, 2021). A study by the *Allgemeiner Deutscher Automobil-Club e.V.* (ADAC) from 2015, last updated in 2019, examined motorbike accident types in a more differentiated manner according to accident causes in combination with riding maneuver and identified "inappropriate speed in curves" as the cause of accidents in 21 % (Pschenitza, 2019).

Compared to passenger cars, the ability of motorbikes to negotiate curves depends to a large extent on the leaning angle built up. As a result, the rider's specific skills play a central role, both physically and mentally. For the further development of active safety systems, it is possible to predict the condition of one's own vehicle using riding dynamics measured variables and taking into account rider influences. On the basis of this prediction, it is possible, for example, to show motorcyclists an individual, optimal approach to a curve before entering it or to improve the skills of the riders with the help of a detailed riding analysis.

In this publication, based on the model presented in (Scherer et. al 2022) for the parameterisation of a motorcyclist's cornering, a first assessment of the applicability of the methodology in road traffic is made. For the modelling, parameterisable mathematical functions are used to describe the speed- and roll angle progression.

The manoeuvre primitives of cornering introduced in (Magiera 2020) are used for this purpose. Every cornering manoeuvre of a motorbike can be divided into a dynamic roll-in and roll-out phase and a quasi-stationary area, similar to a holding phase, when considering the roll angle progressions. The start and end condition of the overall manoeuvre is straight-ahead travel. Here the coefficients used in the nomenclature used in this paper, each lined up as a pair, stand for: R = Right, L = Left, I = In, O = Out.

A special case is the direct transition of a curve into the next curve, in which a right-hand curve goes directly into a left-hand curve, or vice versa, which can result in the combination RL or LR.

The curve combination considered in this paper, consisting of a series of right-hand curves with a transition to a left-hand curve, is shown as an example in Figure 1.

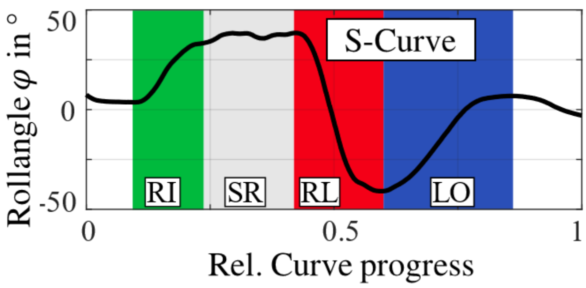

Figure 1 Relative Curve Progress and Maneuver Primitives

For comparability of the results in (Scherer et. al 2022) the so-called curve progression range was introduced. Here, each curve is divided into a start and end point based on the local relationship, and the distance travelled is normalized and distributed locally equidistantly in percentages from 0 to 100%.

The approach of the model used here is to collect measurement data of motorcyclists' riding dynamics, in particular roll angle and speed, which are then transferred into a parameter representation via mathematical approach functions and a curve fitting. The aim of this is making different riders comparable as well as the possibility of reverse transformation into the time domain for the use of the parameters for trajectory prediction. The approach provides that if a curve is passed sufficiently often, a future estimate for the passage of a similar curve can be made.

In (Scherer et. al 2022), two different approach functions for the dynamic and quasi-stationary part of the curve travel are presented. Central variables of consideration are the start and end bounds of the growth functions, the base and gradient values of the linear regression (stationary primitive) and the overlaid oscillations. The nomenclature according to formula (1) is used to separate the coefficients of the two approach functions and to clarify the respective variable.

ISSN: 2667-2812

 http://dx.doi.org/10.59490/6512dbe88ec0d252c9084caa

$$ {}^{i_1}_{i_2}k_{i_3} \tag{1} $$

Here k stands for the coefficient of the approach function. The index i_1 indicates the approximated measured variable (roll angle/ velocity) and the index i_2 contains the information about the considered primitive. If there are several values of the coefficient, this is indicated by the index, this is made clear by the index i_3. Table 1gives an overview of the meaning of the indices.

Table 1. Coefficient Matrice for the approximation functions (Scherer et. al. 2022)

Variable			**Meaning**
k	Coefficient of the approach function	vz	Direction of the growth function
		b	Exponent coefficient of the growth function
		$s_{\mathrm{s}} = vz(a + d)$	Start bound of the growth function
		$s_{\mathrm{e}} = vz(c + d)$	End bound of the growth function
		$base$	Basis of the linear regression
		g	Slope of the linear regression
		$\tilde{a}$	Amplitude of overlaid oscillation
		$\tilde{f}$	Frequency of overlaid oscillation
		$\tilde{l}$	Phase shift of overlaid oscillation
Index			**Meaning**
i_1	Approximated signal	roll	Roll angle signal
		vel	Speed signal
i_2	Primitive	LI/RI	Curve initiation (left/right curve)
		LO/RO	Curve exit (left/right curve)
		LR/RL	Direction change S-curve
		SL/SR	Stationary curve (left/right curve)
i_3	Expression	1	First overlaid oscillation
		2	Second overlaid oscillation
		s	Start (barrier)
		e	End (barrier)

Significant differences between different riders are thus visible in the test track investigations. In contrast to previous scientific approaches with stochastic evaluation of riding ability f.e. in (Magiera, 2020), with the model from (Scherer et. al., 2022) it is possible to interpret measurement data using clear rider-specific parameters, to approximate their course and to compare them across riders.

As in (Scherer et. al. 2022), the following equation (2) is also used in this paper to approximate the dynamic transitions. During the curve initiation, the roll angle is increased from a lower level to a higher level. A logistic growth function is used as an approach, which changes sign depending on the direction of the curve.

$$ f(x) = vz \cdot \left(\frac{a \cdot c \cdot e^{b \cdot x}}{c + a \cdot (e^{b \cdot x} - 1)} + d \right) + \tilde{a} \cdot \sin\left(2\pi \cdot \tilde{f} \cdot \left(x + \tilde{l}\right)\right) \tag{2} $$

The constants a, b and c define the basic shape-influencing parameters of the logistic growth function. Since growth functions cannot map an offset in the solution data, the constant element d is additionally defined, which causes a vertical shift of the function.

The parameters $\tilde{a}$, $\tilde{f}$ and $\tilde{l}$ represent the amplitude, frequency and phase shift of the logistic growth function overlaid oscillation.

The stationary part of cornering typically shows a trend in the roll angle signal. This trend manifests itself in an increase/decrease of the roll angle. In (Scherer et. al. 2022) and also in the current paper a linear regression is used to map this trend. In addition to the trend, there are corrective oscillations, especially in the case of long stationary curves. To take these into account, the first-

ISSN: 2667-2812

 http://dx.doi.org/10.59490/6512dbe88ec0d252c9084caa

degree polynomial is superimposed with two sinusoidal oscillations. These represent the oscillations that occur. Formula (3) shows the approach of the used mathematical approximation, wherin the same nomenclature as in Table 1 provided is used:

$$f(x) = base + g \cdot x \ + \tilde{a}_1 \cdot \sin\left(2\pi \cdot \tilde{f}_1 \cdot \left(x + \tilde{l}_1\right)\right) + \tilde{a}_2 \cdot \sin\left(2\pi \cdot \tilde{f}_2 \cdot \left(x + \tilde{l}_2\right)\right) \tag{3}$$

To calculate the trajectory using the methodology presented in Scherer et.al. (2022), the approximated signals are transformed back into the time domain.

The transverse offset between the estimated and real (measured) trajectory serves as a quality criterion. The estimated trajectory results from the approximated measured data of the roll angle and speed signal, the correction factors due to stationary and dynamic cornering and the manoeuvre distribution. For a more detailed derivation, please refer to (Scherer et. al. 2022).

Methodology

To select suitable curves that match the reference curve presented in Scherer et. al. possible curves were analysed in a radius of 50 km around Frankfurt am Main, Germany.

For the definition of the evaluation curve to prove the transferability of the results from the closed-off test area to the real world, the relationship of the quasi-stationary state at constant cornering between vehicle speed v, curve radius R and the roll angle φ was used. This results in the following relationship, Formula (4:

$$R = -\frac{v^2}{\tan(\varphi) \cdot g} \tag{4}$$

For the evaluation of a motorcyclist's riding abilities, it must be possible under real, good conditions to complete a curve, taking into account the legal limitation, to the limits of riding dynamics. Taking into account the permissible maximum speed on German country roads of v=100 kmh and assuming a theoretical limit roll angle phi=45° at my=1, the following relationship thus results in Table 2:

Table 2. Values for the Reference Curve

Reference Curve Radius		
φ in °	v in km/h	R in m
45 °	40	12.6
	60	28.3
	80	50.3
	100	78.7

This results in a possible, reasonable curve radius between approx. R = 13 m and R = 79 m for German country roads. Curves with a much smaller radius are less suitable for the method presented here, as the low speeds here mean that the quasi-stable range of a typical motorcycle is approached too closely. Especially since it can be assumed that only a few percent of average motorcyclists drive through a curve with near phi =45 °. Additionally, the investigation on the closed track in (Scherer et. al. 2022) was performed with a curve radius of R = 12 m, what is the minimum requirement to the evaluate curve in the real traffic study.

The result of a real-world riding study from (Scherer et. al. 2021) serves as an example here, whereby 75 % of all lean angles are below 25 ° on a typical country road trip in Germany.

In addition to requirements on the curve radius for the particular suitability of the proof of methodology, an important criterion for such a curve is the change in direction that is completed within a curve. This is equivalent to the difference in the vehicle yaw angle between entering and exiting the curve, what can be described as in Formula (5).

$$\Delta\psi = \left|{}^{\mathrm{hor}}\psi_{0\%} - {}^{\mathrm{hor}}\psi_{100\%}\right| \tag{5}$$

ISSN: 2667-2812

 http://dx.doi.org/10.59490/6512dbe88ec0d252c9084caa

A change in direction of at least $\Delta\psi = 90\,°$ must be achieved. Preliminary tests on closed terrain have shown that with a smaller change in direction, the quasi-stationary part of the curve is only present for a very short time or not at all. For comparability with the tests on closed terrain, a $\Delta\psi = 180\,°$ is targeted, as this was the change in direction of the evaluation curve on the closed track in (Scherer et. al. 2022).

In order to be able to exclude vehicle-related influences on the verification, at least two different vehicles should be used in the real-world comparison. In addition, at least two different riding ability levels are necessary for the investigation of the rider's influence. In addition, the influence of external conditions is a focus of the investigation, therefore at least one test person must carry out the test ride several times on days with significantly different boundary conditions (as weather or street conditions).

Influences due to changes between the sterile test environment on the track and rides on the real road must be taken into account. Overall, care must be taken to ensure that the test conditions are as similar as possible, and in particular that the lane width of at least 3 m is maintained.

Measurement Equipment

A Honda CBF 1000 (Figure 2 left) and a BMW K1200 R Sport (Figure 2right) were used for the investigation. Both vehicles are in standard condition, without any modifications or conversions and comply with the German registration regulations.

Figure 2: Motorcycles used for Test Rides

The motorbikes used are clearly distinguished by different chassis concepts (Honda telescopic fork, BMW Duolever), the drive train (Honda chain, BMW cardan) and the power (Honda 98 hp, BMW 163 hp). This is to exclude differences due to the vehicle.

Two measuring devices were used to record the motorbike riding dynamics: a measuring device developed by a student and a WingMan Race from RideLink GmbH. Both devices were validated in advance against a high-precision measuring technique (Automotive Dynamic Motion Analyzer - ADMA from Genesys), whereby inaccuracies in the roll angle of $\varphi = 1°$, the speed $v = 0.5\ \mathrm{m/s}$ and the position in the lane of approx. 1 m must be taken into account when interpreting the results. Both devices have an Inertial Measuring Unit (IMU) including rotation rates, acceleration and magnetic field sensors with a measuring frequency of 100 Hz and a Global Navigation Satellite System signal with a sampling rate of 10 Hz. As visible in Figure 2, the measuring devices were attached to the rear seat of the vehicles and calibrated at the beginning of the measurement rides.

According to the criteria for the selection of an evaluation curve presented in the previous section, a curve combination was selected in the north of Frankfurt on the L3024, at the height of the Windeck parking lot. As shown in **Figure 3**, the curve is approached from the north (point (1) in **Figure 3**) and initially includes a right-hand curve with a radius R = 63 m and a $\Delta\psi = 135°$. At point (2) in **Figure 3**, this changes into a left-hand curve with R = 50 m and a change in direction $\Delta\psi = 110°$. up to point (3). Hereby both partial curves of the total S-combination fulfil the established conditions.

ISSN: 2667-2812

http://dx.doi.org/10.59490/6512dbe88ec0d252c9084caa

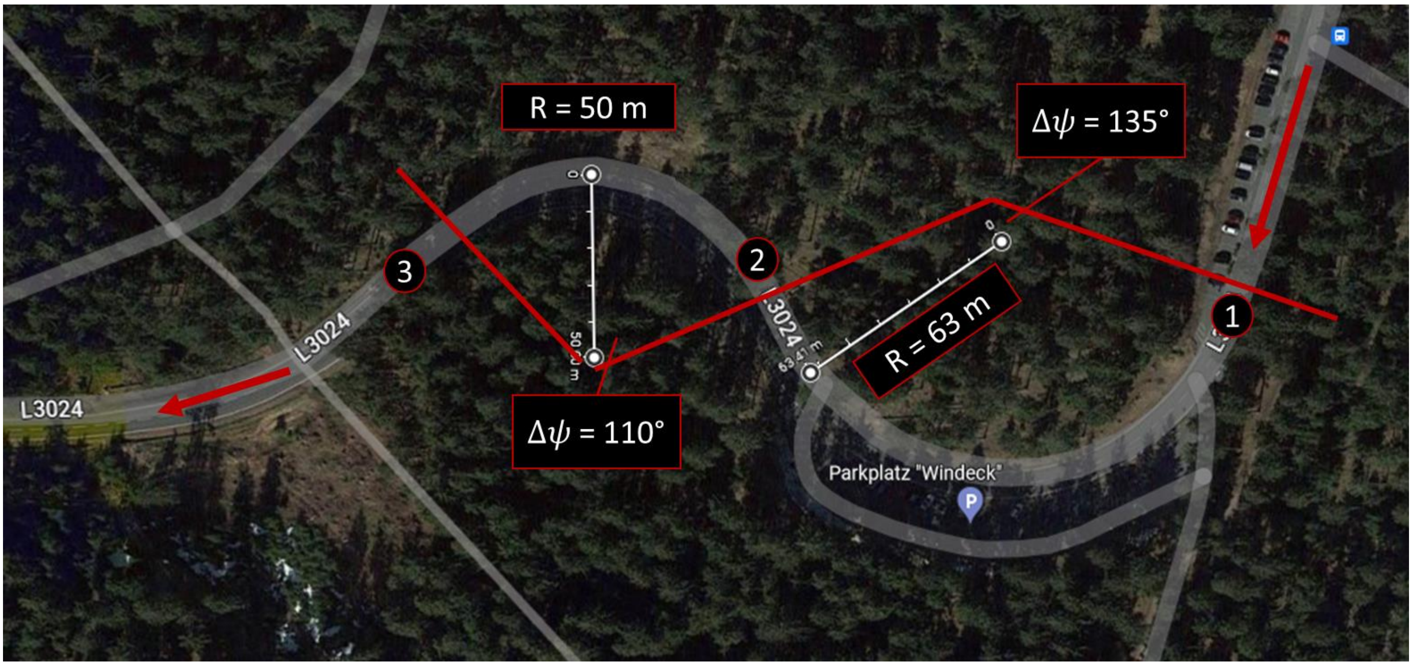

Figure 3. Evaluation Curves for the Real World Investigation

Experiments, Riding Study

The study was conducted on two different days with a total of 4 riders and three vehicles. Due to a faulty installation of the measurement equipment on the vehicle, one data set could not be used for the evaluation and is therefore not discussed further in this publication. Thus, four complete data sets are available for the first proof of the methodology, which does not correspond to any statistical robustness. However, this is not necessary for an initial, random investigation. Each data set contains 5 passes. The given route of a total of 5.2 km with 9 right-hand bends and 11 left-hand bends (one of which corresponds to the evaluation curve) was passed through 5 times in each direction. This results in a total number of n = 40 curve passages, which were used for the further results.

As with the comparison rides on closed track, riding through the entire route served to "familiarise" the riders with the vehicle and the surroundings. The riders did not know in advance what the focus of the study was or, in particular, which curves would be used for the evaluation. The riders were asked to ride within their comfort zone, i.e. not to provoke a particularly risky, but also not a particularly restrained riding style. In addition, the riders were instructed to pause their journey if they ran into other vehicles or if another vehicle appeared behind them, until it was possible to continue on their own again without being influenced by other road users. In addition, the riders were sent into the section of road at an appropriate distance from each other to avoid meeting each other.

The first measurement day was carried out in March 2022 (in the further course marked by the "M" behind the rider number) with the vehicle BMW K1200R (by the abbreviation "B") with rider 1. This part of the study aims to compare different environmental influences. On the day of the measurement, the outside temperature was 6°C, the road conditions were dry, the sky was overcast. The second measurement day on which all riders, i.e. rider 1 again, rider 2 and rider 3 drove the measurement routes for the first time was carried out in July 2022 with an outside temperature of 30°C, sunshine and very good and dry road conditions.

Table 3: Riders Age, Yearly km and Experience for Real World Study

Rider					
Rider Nr.	Motorcycle	Age	Yearly km	Experience	Season
1MB	BMW	32	4000	Experienced	First Ride
1JB	BMW	32	4000	Experienced	Well Practice
2JH	HONDA	31	500	Beginner	First Ride
3JH	HONDA	29	5000	Experienced	Well Practice

ISSN: 2667-2812

http://dx.doi.org/10.59490/6512dbe88ec0d252c9084caa

Table 3 lists the characteristics of the riders and vehicles, as well as the respective seasonal influence. Rider 1 and rider 3 are experienced frequent riders with a high annual mileage, whereas rider 2 has riden less than 1000 km since receiving the riding licence and the last active trip was years ago.

Thus, the results in the comparison of rider 1 are representative for the investigability of seasonal differences, the comparison between rider 1 and rider 3 with otherwise similar riding behaviour for the influence of different vehicles and the difference between rider 1 or rider 3 and rider 2 for the influence by riding experience or also riding ability in general.

Results

For a first general impression, the complete roll angle and speed curves of all runs are first analysed. Figure 4 in the top left-hand corner shows the roll angle curves for each rider and also separately for the March (blue) and July (red) runs.

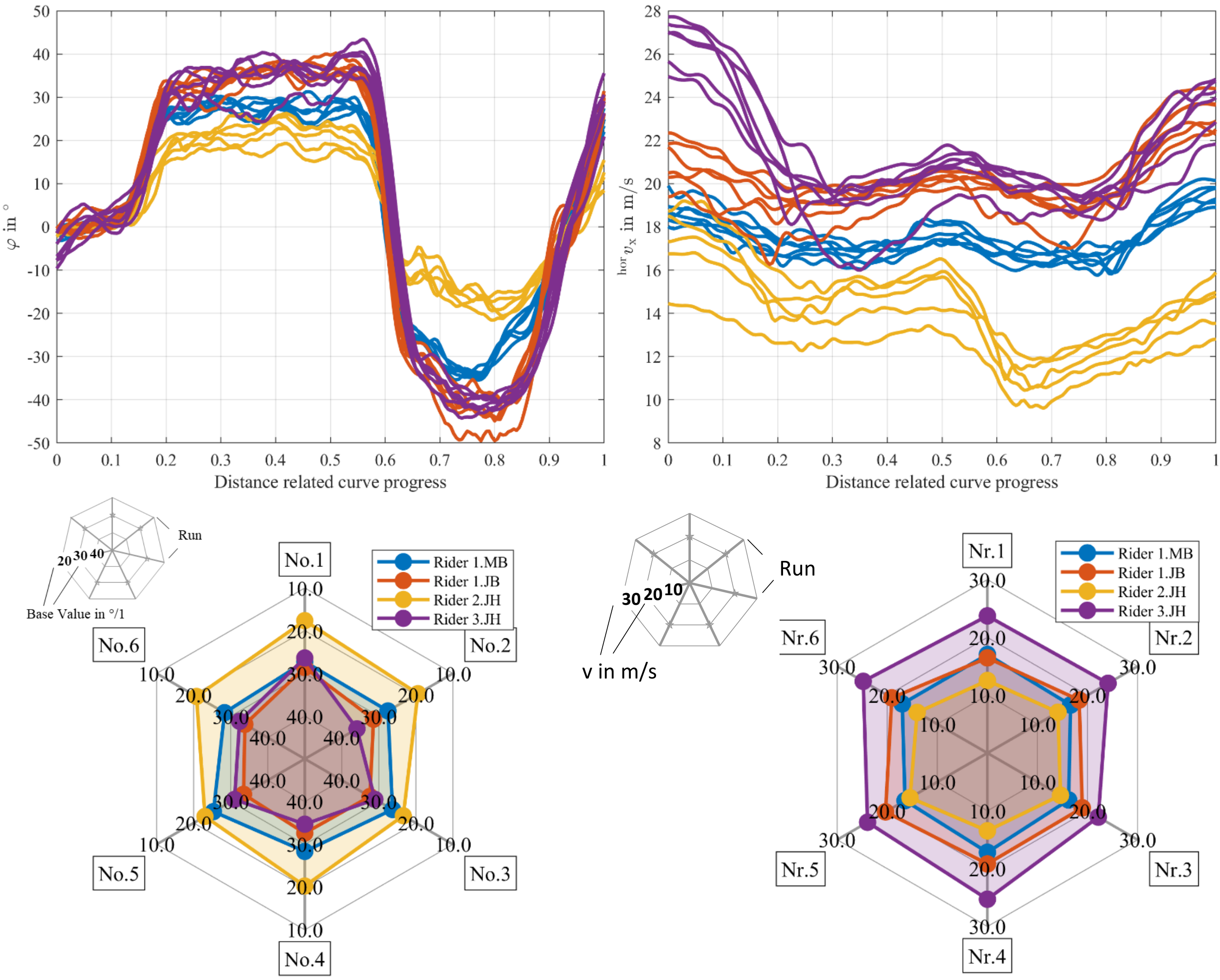

Figure 4. Top: left: roll-angle, right velocity over curve progress, down: left base Roll angle, left in velocity

The roll angle remains relatively stable for a single rider across different experiments. However, it's clear that roll angles differ significantly between distinct riders, emphasizing the unique nature of each rider's control style.

ISSN: 2667-2812

 http://dx.doi.org/10.59490/6512dbe88ec0d252c9084caa

When riders share similar experience levels and practice under comparable seasonal conditions, their roll angle profiles closely align. This consistency highlights the role of both experience and seasonal practice in shaping roll angle patterns. Notably, riders with more experience tend to exhibit higher baseline roll angle values, visible in Figure 4, down left for the base values of the quasi-stationary right cornering phase. Seasonal variations lead to changes in total roll angle values, but the underlying patterns persist. This suggests that seasonal factors may affect the magnitude of roll angles while leaving the fundamental roll angle behaviour across riders largely intact.

Velocity profiles exhibit significant disparities between different riders, with noticeable differences emerging, especially at the beginning of curves, visible in Figure 4 on the right. This underscores the significant impact of individual rider preferences and control strategies on velocity changes. High levels of rider experience or training are associated with elevated velocity profiles. This finding suggests that seasoned riders navigate curves at higher speeds, reflecting their enhanced control and confidence. In the stationary curve segments of the velocity profiles, we observe striking similarity among riders with similar experience and training levels. This underscores how these factors contribute to maintaining consistent velocity during stable riding conditions. Seasonal variations result in lower overall velocity values. However, the fundamental velocity patterns remain consistent, indicating that seasonal conditions may influence velocity magnitude without altering the underlying velocity trends.

Looking at the development of the roll angle gradient during the quasi-stationary right cornering, a slightly different pattern becomes visible in Figure 5.

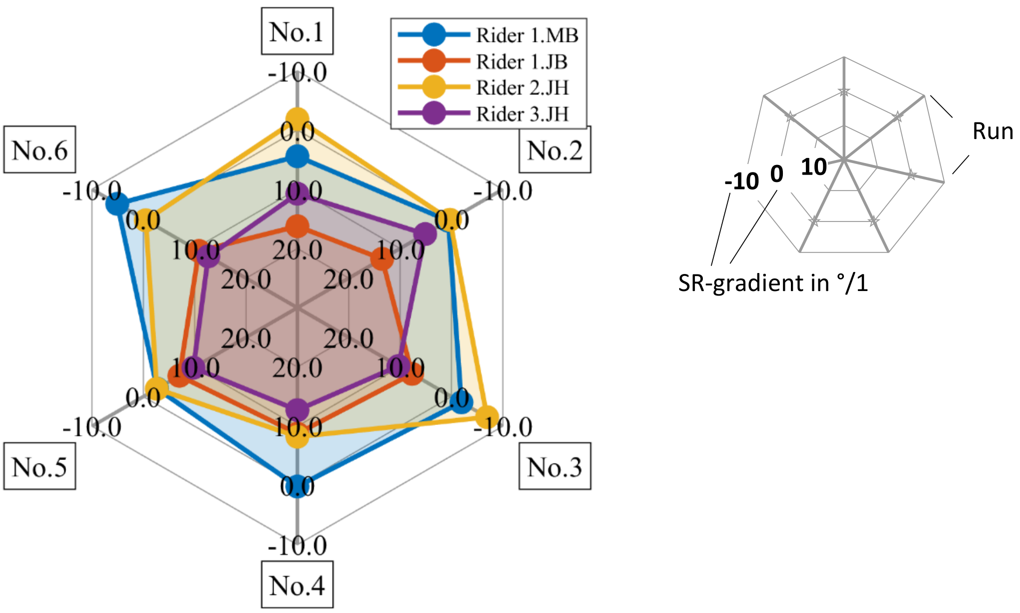

Figure 5. Stationary Right Gradient of all Riders

Here it is noticeable that the experienced rider 1 in March shows a similar behaviour in unfavourable weather and road conditions as the inexperienced rider 2 in very good conditions. A gradient close to zero or in the negative range stands here for very defensive cornering, a reduction in lean angle over the cornering course.

With the experienced riders 1.JB and 3.JH a quite similar behaviour is observed in good conditions. A build-up of lean angle over the course of the curve can be observed. However, the riders differ more on the first two runs than from the third run onwards. Here, for example, a kind of habituation effect to the curve may occur after repeated riding. It is noticeable that none of the riders constantly increases from pass to pass, which was a possible assumption at the beginning of the study.

As described in equation (3), the linear regressive part of the approximation is superimposed by two oscillation parts. In the current paper only the first superimposed oscillation is handled, as for the second one there are no significant insights visible.

ISSN: 2667-2812

 http://dx.doi.org/10.59490/6512dbe88ec0d252c9084caa

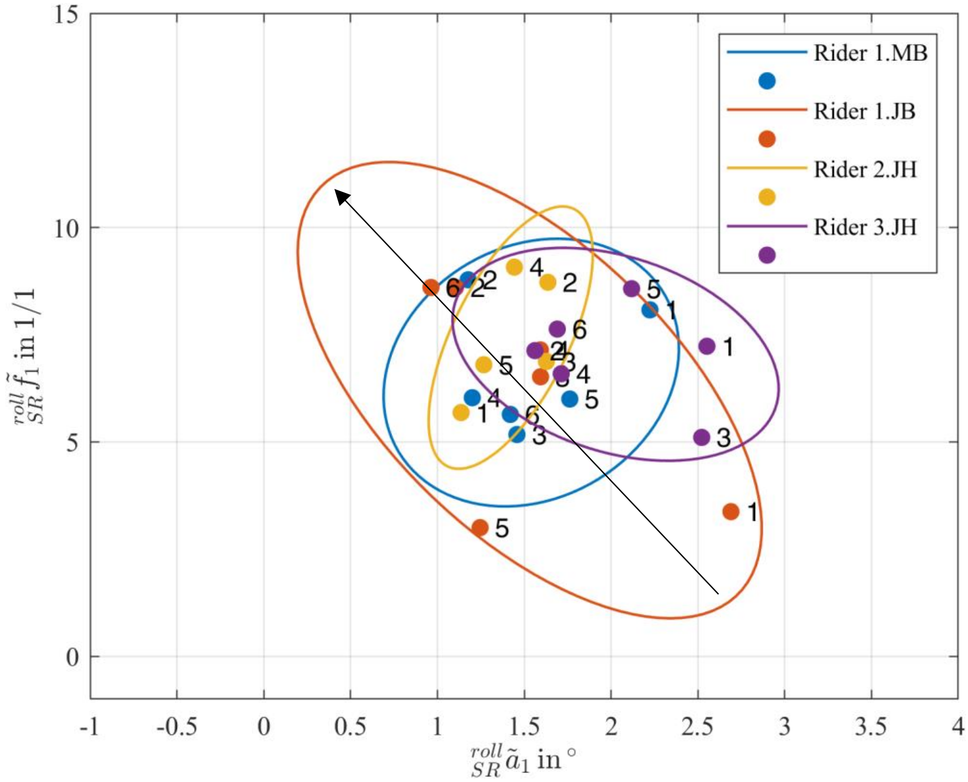

Figure 6. Pairing of Coefficients of Amplitude ($\tilde{\mathbf{a}}_\mathbf{1}$) und frequency ($\tilde{\mathbf{f}}_\mathbf{1}$) in a $\mathbf{90}\%$ confidence intervall

The pairs of coefficients from the amplitude and frequency of the first superimposed oscillation, shown in Figure 6, give a sense of the way in which the lean angle is maintained or changed in a stable manner, for example in the quasi-stationary phase. During the tests on closed-off terrain, a correlation was found in particular between the alignment of the ellipses (shown here with a confidence interval of 90 %) and the riding skill. This cannot be demonstrated with the sample size shown here. A difference is visible, but cannot be attributed to any of the influencing variables.

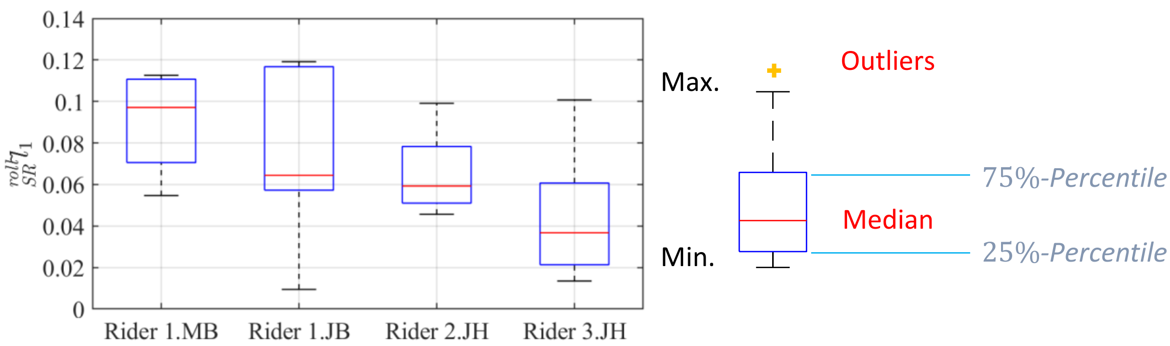

Figure 7. Phase shift of the first superimposed oscillation

The same applies to the phase shift of the first oscillation. Here, as can be seen in Figure 7, no distinction is possible between the three riders considered.

Due to the number of coefficients examined, the results of the remaining variables are summarised in the Table 4.

ISSN: 2667-2812

 http://dx.doi.org/10.59490/6512dbe88ec0d252c9084caa

Table 4. Comparison of all coefficients betweem real world and closed track investigation

Coefficient type	Curve	Primitivee	Coefficient	Realworld	Closed-Track
Roll angle coefficient	180°-right corner	SR-Primitive	Gradient	yes	yes
			Base Value	yes	yes
			Correction amplitude and frequency first overlaid vibration	yes	yes
			Phase displacement first overlaid vibration	no	no
			Correction amplitude and frequency second overlaid vibration	partially	yes
			Phase displacement second overlaid vibration	partially	partially
		RI-Primitive	Start borders	partially	yes (but LI-Primitive)
			End borders	yes	yes (but LI-Primitive)
			Exponent coefficient	no	yes
			Correction amplitude and frequency overlaid vibration	no	yes
		RO-Primitive	Start borders	yes	yes
			End borders	no	yes
			Exponent coefficient	no	yes
			Korrekturamplitude und -frequenz überlagerte Schwingung	no	no
	S-Curve	SL-Primitive	Gradient	no	not recorded
			Base value	partially	not recorded
			Correction amplitude and frequency first overlaid vibration	no	not recorded
		RL-Primitive	Correction amplitude and frequency overlaid vibration	no	not recorded
		LO-Primitive	Correction amplitude and frequency overlaid vibration	no	not recorded
Velocity coefficients	180°-Right corner	RI-Primitive	Start borders	yes	yes (but LI-Primitive)
			End borders	yes	yes (but LI-Primitive)
			Korrekturamplitude und -frequenz überlagerte Schwingung	no	yes (but LI-Primitive)
			Vorzeichen	no	partially (but LI-Primitive)
		SR-Primitive	Gradient	no	anders analysiert
			Base value	yes	not recorded
			Correction amplitude and frequency first overlaid vibration	no	no (but SL-Primitive)
			Correction amplitude and frequency first overlaid vibration und Base value	yes	yes (but SL-Primitive)
		RO-Primitive	Startschranken	yes	yes (but LO-Primitive)
			End borders	yes	yes (but LO-Primitive)
			Exponent coefficient	yes	yes (but LO-Primitive)
			Sign	no	no (but LO-Primitive)
	S-Curve	SL-Primitive	Gradient	yes	not recorded
			Base value	yes	not recorded

As described in the introduction, with the help of the coefficients approximated in this study, a backward transformation into the time domain and, resulting from this, a future position of the motorbike can be estimated by calculating a yaw rate from the roll angle and speed characteristics. Corresponding trajectories were calculated for all three riders by using the mean values of the coefficients. As an example, the result of the estimation with the largest deviation is shown in Figure 8.

ISSN: 2667-2812

http://dx.doi.org/10.59490/6512dbe88ec0d252c9084caa

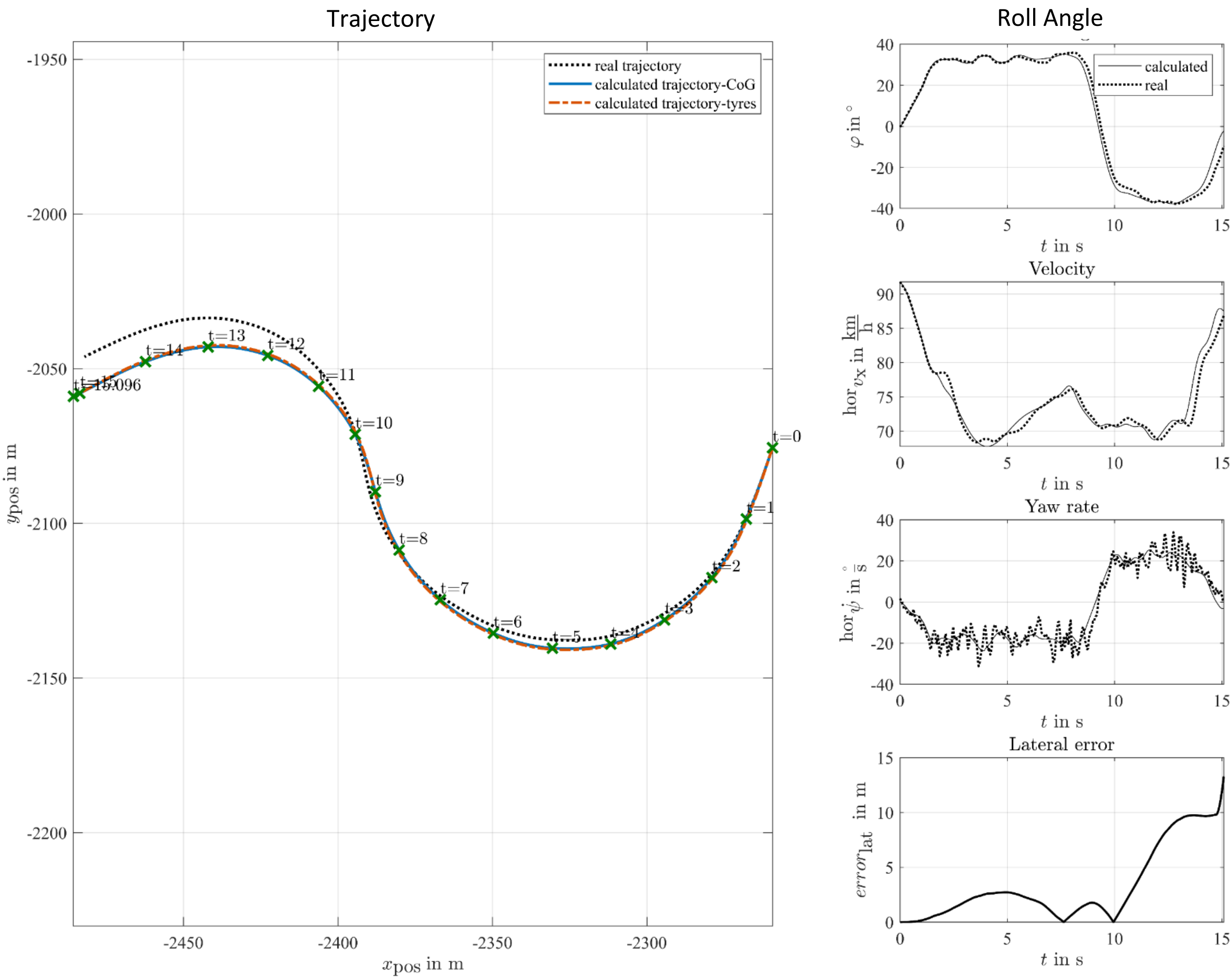

Figure 8. Trajectory prediction, comparing measurements and estimation, left x and y in a reference coordinate system, right from the top: roll angle, velocity, yaw rate and lateral error over time

The disparity between the estimated and measured trajectories reaches its peak, with a lateral deviation of 3 meters occurring at t = 5 seconds. This error gradually diminishes until the transition into the opposite curve, only to resurge and reach its maximum magnitude at t = 15 seconds, resulting in a lateral deviation of 12 meters. Notably, the most significant estimation error manifests during the transition into the opposite curve. The model demonstrates high predictive accuracy for future positions, with more than 85% of maneuvers exhibiting a lateral deviation of less than 2%. This affirms its effectiveness in real-world conditions, validating its utility beyond the closed terrain testing outlined in (Scherer, 2022).

Particularly noteworthy is the phase following the completion of the first curve segment, where the estimated trajectory, accounting for the measurement inaccuracies of the GNSS system, falls within a range that allows us to distinguish between staying within the lane and successfully navigating the corner without incident.

ISSN: 2667-2812

http://dx.doi.org/10.59490/6512dbe88ec0d252c9084caa

Discussion and Outlook

The aim of this study was the investigation of the applicability of a motorcycle rider model from a closed test track, with a particular focus on roll angle and velocity profiles and the usability for trajectory prediction. While the investigation was constrained by a limited number of measurements conducted on chosen evaluation curves involving three riders, it has yielded valuable insights. Notably, rider experience, training, and seasonal conditions play pivotal roles in shaping both roll angle behaviour in quasi-stationary phases and velocity trends. These insights underline the importance of considering individual rider characteristics in the development of motorcycle safety systems. However, it is worth noting that not all the observations of the closed-track tests could be unequivocally confirmed, especially regarding superimposed oscillations, which did not exhibit the same level of specificity as the other parameters. The trajectory prediction performed by means of the back-transformed parameterised coefficients yielded an error in the form of the lateral deviation between measurement and estimation of less than 2% in more than 85% of all maneuver after the first curve passage.

Looking ahead, there is significant potential for further exploration in this field. A crucial next step would involve a comprehensive statistical validation of the presented method. By expanding the dataset and employing robust statistical techniques, the reliability and generalizability of these findings could be approved. Furthermore, future research could explore the development of tailored motorcycle safety interventions based on the rider-specific insights gained in this study. These interventions could aim to enhance rider safety and reduce the risk of accidents by accounting for individual rider characteristics, experience levels, and seasonal conditions.

In summary, this study lays a foundation for a deeper understanding of motorcycle rider behaviour, opening the door to more effective safety measures. As the extension of knowledge in this domain continues, in the future tailored safety systems and interventions will contribute significantly to improving motorcycle safety on the road.

References

Destatis, (2021) Verkehrsunfälle, Statistisches Bundesamt, Germany

Magiera, N, (2020) Identifikation des Fahrfertigkeitsniveaus von Motorradfahrern in Kurvenfahrt im Realverkehr, *Dissertation*, TU Darmstadt, Germany

Pschenitza, M. (2019), Auswertung von Motorradunfällen: Konstellationen, Besonderheiten, Abhilfemaßnahmen. *Berichte der ADAC Unfallforschung*, Landsberg am Lech, Germany

Prokop, G., Hannawald, L., Köbe, M. (2017, April), Szenarien-basierte Plattform zur Inspektion automatisierter Fahrfunktionen - Eine Bewertungsmethodik zur Inspektion automatisierter Fahrfunktionen. *Proceedings, Symposium für Unfallforschung und Sicherheit im Straßenverkehr der ADAC Stiftung*, Munich, Germany, 115-127

Scherer, F., Basten, T. (2022, October 03-04), Development of a motorcyclist model for trajectory prediction. *Proceedings, 14th International Motorcycle Conference 2022*, Cologne, Germany, 265-299

Scherer, F.; Winner, H.; Pleß, R.; Will, S; Neukum, A.; Stanglmaier, M.; Bäumler, M.; Siebke; C.; Prokop, G.; (2021, November), Schräglagenangst. *Berichte der Bundesanstalt für Straßenwesen, F142*, Bergisch-Gladbach, Germany

ISSN: 2667-2812